Helical Wrapping of Single-Walled Carbon Nanotubes by Water Soluble Poly(p-phenyleneethynylene)

ARTICLE *in* NANO LETTERS · MAY 2009

Impact Factor: 13.59 · DOI: 10.1021/nl8032334 · Source: PubMed

NANO LETTERS

2009
Vol. 9, No. 4
1414-1418

Helical Wrapping of Single-Walled Carbon Nanotubes by Water Soluble Poly(*p*-phenyleneethynylene)

Youn K. Kang,[†,‡] One-Sun Lee,[†] Pravas Deria,[†,||] Sang Hoon Kim,[§] Tae-Hong Park,[†] Dawn A. Bonnell,[*,§] Jeffery G. Saven,[*,†] and Michael J. Therien[*,||]

Department of Chemistry, University of Pennsylvania, 231 South 34th Street, Philadelphia, Pennsylvania 19104, Division of Chemistry and Molecular Engineering, Department of Chemistry, College of Natural Sciences, Seoul National University, Seoul 151-747, Korea, Department of Materials Science and Engineering, University of Pennsylvania, 3231 Walnut Street, Philadelphia, Pennsylvania 19104, and Department of Chemistry, French Family Science Center, 124 Science Drive, Duke University, Durham, North Carolina 27708

Received October 26, 2008; Revised Manuscript Received January 13, 2009

ABSTRACT

Amphiphilic, linear conjugated poly[*p*-{2,5-bis(3-propoxysulfonicacidsodiumsalt)}phenylene]ethynylene (PPES) efficiently disperses single-walled carbon nanotubes (SWNTs) under ultrasonication conditions into the aqueous phase. Vis-NIR absorption spectroscopy, atomic force microscopy (AFM), and transmission electron microscopy (TEM) demonstrate that these solubilized SWNTs are highly individualized. AFM and TEM data reveal that the interaction of PPES with SWNTs gives rise to a self-assembled superstructure in which a polymer monolayer helically wraps the nanotube surface; the observed PPES pitch length (13 ± 2 nm) confirms structural predictions made via molecular dynamics simulations. This work underscores design elements important for engineering well-defined nanotube-semiconducting polymer hybrid structures.

Despite the extraordinary optical,[1−5] electronic,[6,7] electrical,[8−12] and mechanical[13−17] properties of single-walled carbon nanotubes (SWNTs),[18,19] the notorious insolubility of these structures that derives from strong intertube van der Waals interactions[20,21] limits their full utilization in materials and devices. Perhaps the most exploited method to overcome this obstacle relies upon ultrasonication enforced segregation of nanotube strands out of entangled bundles, followed by SWNT surface noncovalent[22] or covalent chemical functionalization. Preserving key optical, electrical, and structural properties of SWNTs requires noncovalent solubilization strategies; a wide-range of surfactants, small molecules, and polymers have been utilized for this purpose and have been the subject of a recent review by Tasis and Prato.[23] Among these agents, polymers offer the potential to evolve new functional materials through well-defined SWNT-polymer interactions. Flexible polymers, congruent with intuition, provide structures capable of wrapping the SWNT surface, facilitating dispersion.[24−28] Conjugated polymer-SWNT blends often exhibit synergistic optoelectronic effects; for example, it has been established that such compositions can manifest dramatically enhanced conductivities and charge mobilities.[29−33] Of these materials, it has been established that poly(*m*-phenylenevinylene) (P*m*PV) helically wraps SWNTs.[27,34] Related work reports that poly(*p*-phenyleneethynylene) (PPE) interacts with the nanotube surface in a parallel mode and plays a role in assembling a ribbon-type super structure of SWNTs;[35] in contrast, in situ polymerization of phenylacetylene in the presence of nanotubes suggests the formation of helical polymer-SWNT structures.[24] Further, recent works have established that regardless of morphology, linear, conformationally restricted conjugated polymers can function as dispersing agents that solubilize SWNTs in the nonaqueous phase.[36−38] While it is widely accepted that conjugated polymers bind SWNT surfaces through $\pi-\pi$ interactions, there remains a general need to establish rules and principles that guide the assembly of individualized SWNT-semiconducting polymer structures having a well-defined morphology.

Water-soluble poly[*p*-{2,5-bis(3-propoxysulfonicacidsodiumsalt)}phenylene]ethynylene (PPES, shown in Chart

* To whom correspondence should be addressed. (D.A.B.) Tel: +215-898-6231. Fax: +215-746-3204. E-mail: bonnell@lrsm.upenn.edu. (J.G.S.) Tel: +215-573-6062. Fax: +215-573-0980. E-mail: saven@sas.upenn.edu. (M.J.T.) Tel: +919-660-1670. Fax: +919-660-1605. E-mail: michael.therien@duke.edu.

[†] Department of Chemistry, University of Pennsylvania.

[‡] Seoul National University.

[§] Department of Materials Science and Engineering, University of Pennsylvania.

[||] Duke University, Durham.

10.1021/nl8032334 CCC: $40.75
Published on Web 03/12/2009

Chart 1. The Structure of PPES

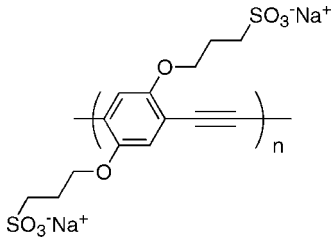

1), synthesized from {[2,5-diiodo-1,4-bis(3-propoxysulfonicacid)benzene] sodium salt} and [1,2-bis(4′,4′,5′,5′-tetramethyl[1′,3′,2′]dioxaborolan-2′-yl)ethyne] via Suzuki-Miyaura polycondensation,[39] is an amphiphilic polyelectrolyte consisting of a linear conjugated PPE backbone and two negatively charged side groups for every phenyl unit. Given the established performance of amphiphilic structural motifs for the dispersion of SWNTs at high mass percent conversion[40] in the aqueous phase,[1,28,41−43] and the substantial $\pi-\pi$ interactions provided by the aryleneethynylene repeat unit, aqueous phase SWNT solubilization via PPES was interrogated. This work shows that PPES forms a helical superstructure upon associating with SWNTs, despite its intrinsic linear, conformationally restricted nature, and provides substantial aqueous phase solubility.

The extent to which a fixed SWNT mass (HipCo tubes batch 81) becomes suspended in aqueous solution (the mass percent conversion) by PPES (see Supporting Information for polymer characterization data) was estimated by examination of electronic absorption oscillator strengths over a 600−1600 nm wavelength range, referenced to established literature benchmarks,[28,43,44] where the oscillator strength of a maximally concentrated sodium dodecylsulfate (SDS) suspended SWNT sample (SDS-SWNT) was taken to be 1 (Figure 1a). Among a number of varied experimental parameters, the sonication time was found to be the most important factor that determined the mass percent conversion. Resasco has shown previously that the concentration of dispersed SWNTs using a sodium dodecylbenzenesulfonate (SDBS) surfactant increased with increasing sonication time, reaching a maximum value at ∼1 h;[44] similar to this result, the relative oscillator strengths of PPES-SWNT suspensions increased 3-fold over a 30 (0.68) to 60 min (2.05) sonication period (Supporting Information, Figure S1). It is important to note, however, that longer PPES sonication times are required to fully exfoliate SWNT bundles relative to that required by common surfactants such as SDBS. In these studies, a maximum SWNT concentration in water was obtained after ∼3 h of sonication; note that the relative SWNT absorptive oscillator strength of this PPES-SWNT sample is nearly 1 order of magnitude greater than that evident in the fully saturated SDS-SWNT benchmark. The maximum mass percent conversion[40] for this PPES-SWNT sample was ∼70%, following centrifugation at 36 000 g for 3 h.[45]

The vis-NIR absorption spectral features of PPES-SWNT suspensions (Figure 1) show two interesting features relative to that for the SDS-SWNT benchmark. First, PPES-SWNT suspensions exhibit bathochromic shifts in both first and second subband regions; note that the magnitude of these

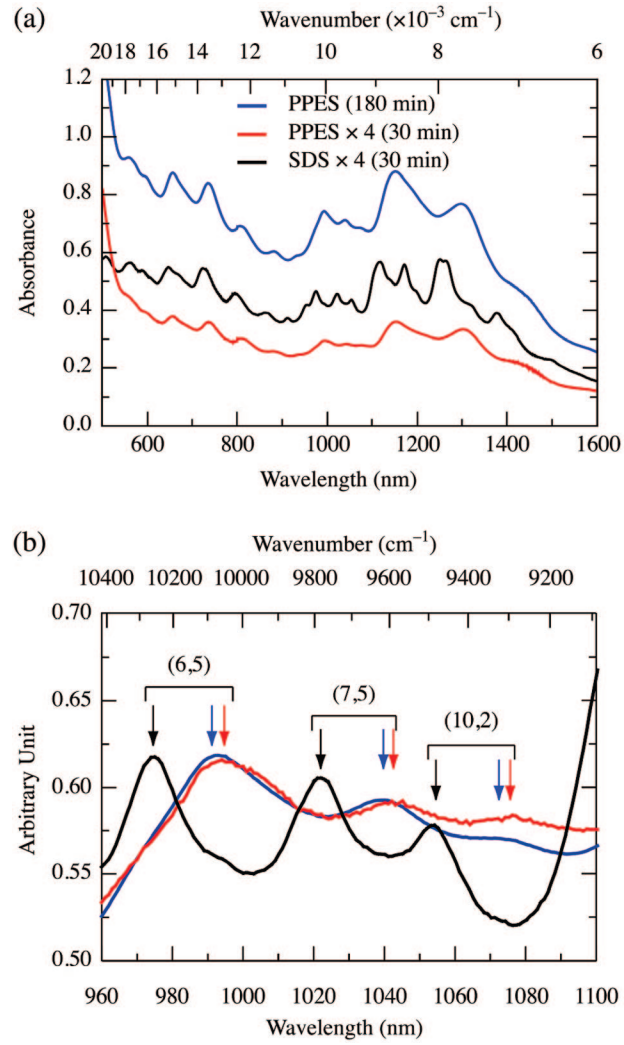

Figure 1. (a) Vis-NIR absorption spectra of PPES-SWNT and SDS-SWNT samples. Optical path length = 1 mm. Note that the spectrum of the PPES-SWNT (30 min sonication time) and SDS-SWNT (saturated) samples are scaled by a factor of 4. (b) NIR spectra of SDS-SWNT (saturated, black) and PPES-SWNT (30 min sonication time, red; 180 min sonication time, blue) samples normalized at the (6,5) absorption peak maximum. Arrows indicate relative peak positions, which highlight the degree of PPES-SWNT absorptive bathochromic shifts relative to corresponding transitions in the SDS-SWNT benchmark spectrum.

spectral red shifts for the prominent absorption maxima evident in the Figure 1b manifold of states is ∼200 cm^{-1}. Second, there is an apparent spectral line broadening in the first subband region. Since it is commonly accepted that a significant concentration of small SWNT bundles causes spectral line broadening and modest absorption band bathochromic shifts relative to the electronic spectra corresponding to samples of highly individualized tubes,[1,46] one interpretation for these results is that the PPES-SWNT samples feature a smaller fraction of individual nanotubes relative to the SDS-SWNT reference suspension.

To probe the structure of PPES-SWNTs and assess the extent to which the above-noted samples are composed of individualized tubes, a range of microscopy experiments was carried out. Figure 2a,c displays atomic force microscopy (AFM) images of PPES-SWNTs; note that the Figure 2c

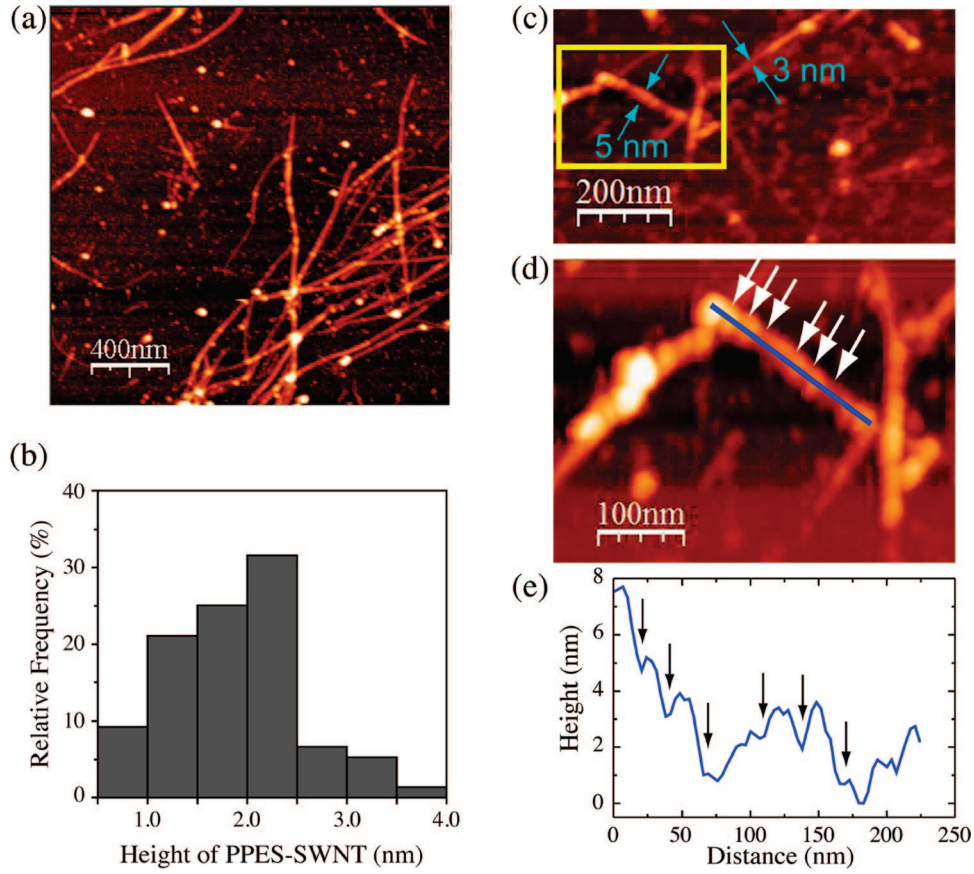

Figure 2. (a) Topographic AFM image of PPES-SWNTs. Experimental conditions: sonication time = 3 h; Si surface; tapping mode; see Supporting Information for further details. (b) PPES-SWNT height profile histogram of the panel a data. (c) Topographic AFM image of PPES-SWNTs (sonication time = 30 min) on a mica surface pretreated with NH_4Cl, highlighting the thicknesses of two solubilized tubes. For height profiles and additional experimental details, see the Supporting Information. (d) Enlarged view of the area in the yellow box in panel c. (e) Height profile along the blue line in panel d showing the periodic height oscillation that derives from PPES helical wrapping of the SWNT.

image, which probes structures derived from a 30 min sonication time, shows that the PPES-SWNT height profile ranges from 3−5 nm. These data stand in sharp contrast to the image corresponding to a 3 h sonication time (Figure 2a), which underscores that ∼86% of observed tubes possess height profiles less than 2.5 nm (Figure 2a,b). Considering the fact that the average diameter of a HipCo tube is ∼1 nm[46,47] and that the encapsulating, heavily substituted PPES polymer is expected to augment the observed diameter by several Ångstroms, the height profile data compiled in Figure 2b indicate clearly that more than 80% of dispersed PPES-SWNTs are individualized.

It should be noted that while the spectral peak positions of the semiconducting (6,5), (7,5), and (10,2) tubes highlighted in the overlaid spectra of Figure 1b show apparent bathochromic shifts and line broadening for both PPES-SWNT samples relative to the SDS-SWNT point of reference, it is apparent that sonication time has little impact upon PPES-SWNT peak positions and absorption band spectral breadths (Figure 1b);[48] this result indicates that differences between PPES-SWNT and SDS-SWNT spectra do not derive primarily from differences in the relative fractions of small nanotube bundles present. Early work by Smalley revealed that the addition of polyvinylpyrrolidone (PVP) to SDS-dispersed SWNTs caused the absorptive transitions beyond 900 nm to red shift and broaden;[1] likewise, single strand DNA-solubilized SWNTs exhibit characteristic spectral bathochromic shifts and line broadening.[28,49] Interestingly, a close examination of the absorption spectra of these DNA-suspended SWNT samples (DNA-SWNTs) shows that the NIR transitions for the semiconducting (6,5), (7,5), and (10,2) tubes exhibit peak positions similar to those evident for the PPES-SWNT samples. Congruent with the data summarized in Figures 1 and 2, these studies point to band gap energy perturbation deriving from the strong $\pi-\pi$ interaction of these highly conjugated polymeric surfactants and the SWNT surface as the primary driving force for the bathochromic shifts and line broadening evident in PPES-SWNT and DNA-SWNT spectra relative to that for the SDS-SWNT benchmark.

To obtain further insight into the PPES-SWNT structure and help elucidate the nature of the PPES/SWNT complex, a molecular dynamics (MD) simulation that probed the interaction of a (10,0) nanotube with a PPES 20-mer was carried out (NAMD,[50] CHARMm[51] force field, total time of 20 ns, explicit water and counterions; initial configuration: SWNT and PPES aligned parallel, with the polymer and nanotube surface separated by 4 Å. Computational details are provided in the Supporting Information). Snapshots from the MD simulation are shown in Figure 3a. Despite the fact that the PPES 20-mer and the (10,0)-SWNT were aligned in a parallel initial

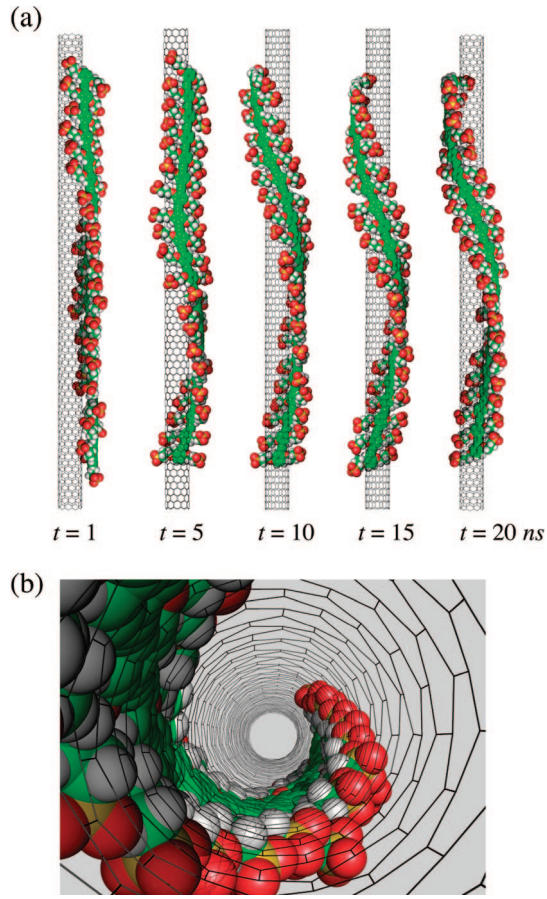

Figure 3. (a) Snapshots of the interaction process between a (10,0)-SWNT and a PPES 20-mer obtained through MD simulation obtained over a 1−20 ns period. The PPES helix pitch approached an equilibrium value of 14 ± 1 nm after ∼15 ns. Water molecules have been omitted for clarity. (b) View along the nanotube axis of the PPES/SWNT complex at $t = 20$ ns of MD simulation. Note that the phenyl ring and ethyne component of each arylethynyl monomeric unit contacts the SWNT cylinder, while the negatively charged sulfonate groups are displaced slightly above SWNT surface.

configuration, the PPES oligomer began to wrap the SWNT at ∼10 ns, forming a helical structure. After 15 ns of MD simulation, the PPES-SWNT complex reached its equilibrium structure, which evinced a PPES helical pitch of 14 ± 1 nm (Supporting Information, Figure S9). These computations indicate that the binding energy difference between the parallel and helical PPES/SWNT conformations is 1.1 kcal/mol/monomer (Supporting Information, Figure S10) and underscore that the total energy stabilized via the polymer helical wrapping interaction accumulates as the number of unit monomers increases. As the experimentally determined, average degree of polymerization for the PPES utilized in this study was 47, a helical wrapping mode augments the binding energy by ∼52 kcal/mol relative to the parallel geometry.

The helix radius formed by the PPES 20-mer in the MD simulation of the PPES/SWNT interaction was determined to be 7.36 ± 0.03 Å at equilibrium. Considering the fact that the radius of a (10,0)-SWNT is known to be 3.97 Å,[47] the distance between the PPES backbone and the surface of the nanotube

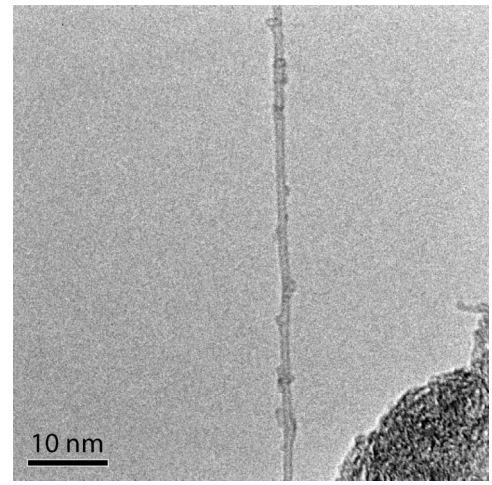

Figure 4. TEM image of a PPES-SWNT.

corresponds to 3.39 ± 0.03 Å, consistent with an optimal van der Waals interaction between PPES and SWNT.

The structure of PPES-SWNT predicted by MD simulation was confirmed by TEM and AFM. In Figure 4, the TEM image shows unmistakably the helical wrapping structure of PPES-SWNT complex; note that small bulges on one side of the tube are mirrored by companion protuberances on the other with a clear lateral shift of ∼5 nm. This pattern repeats at 13 ± 2 nm intervals along the SWNT axis, remarkably close to the equilibrium helical pitch (14 ± 1 nm) predicted by MD simulation.[52] Along these lines, note that the AFM study highlighted in Figure 2d and its corresponding height profile analysis are congruent with the PPES-SWNT helical wrapping arrangement evident in the TEM. The periodic wavelike height profiles apparent in these microscopy experiments are reminiscent of data reported by Shinkai, which showed a similar recurring height profile dependence for SWNTs helically wrapped by a polysaccharide.[53]The PPES-SWNT structure reported herein contrasts results reported by Rice and co-workers, who utilized a related *p*-phenyleneethynylene-based polymer as a SWNT dispersing agent, but did not realize periodic nanotube helical wrapping.[36]

In sum, this work demonstrates that: (i) PPES, a linear, conformationally restricted conjugated polymer, disentangles SWNT strands from their bundled forms at high mass percent conversion, providing suspensions where ∼80% of the solubilized tubes are individualized at a concentration that exceeds by an order of magnitude that provided by the SDS-SWNT benchmark; (ii) in contrast to previous studies in which other *p*-phenyleneethynylene-based polymers have been shown to interact with SWNTs in a parallel fashion, PPES wraps SWNTs forming a self-assembled helical super structure; and (iii) the experimentally observed PPES-SWNT helical pitch of 13 ± 2 nm is in close agreement to the 14 ± 1 nm value predicted by MD simulation. Given that conjugated polymer-SWNT blends often exhibit synergistic optoelectronic effects, this work may help guide the super-helical assembly of SWNTs with other technologically important, linear semiconducting polymers.

Acknowledgment. This work was supported by a grant from the Office of Naval Research (N00014-06-1-0360). The

authors thank the MRSEC (DMR-00-79909) and NSEC (DMR-0425780) Programs of the National Science Foundation for infrastructural support. M.J.T. is grateful to the Flemish Academy of Arts and Sciences (VLAC) and the Francqui Foundation (Belgium) for research fellowships.

Supporting Information Available: PPES-SWNT preparative procedure, TEM and AFM experimental details, computational methodology. This material is available free of charge via the Internet at http://pubs.acs.org.

References

(1) O'Connell, M. J.; Bachilo, S. M.; Huffman, C. B.; Moore, V. C.; Strano, M. S.; Haroz, E. H.; Rialon, K. L.; Boul, P. J.; Noon, W. H.; Kittrell, C.; Ma, J. P.; Hauge, R. H.; Weisman, R. B.; Smalley, R. E. *Science* **2002**, *297*, 593–596.

(2) Bachilo, S. M.; Strano, M. S.; Kittrell, C.; Hauge, R. H.; Smalley, R. E.; Weisman, R. B. *Science* **2002**, *298*, 2361–2366.

(3) Lefebvre, J.; Homma, Y.; Finnie, P. *Phys. Rev. Lett.* **2003**, *90*, 217401.

(4) Wang, F.; Dukovic, G.; Brus, L. E.; Heinz, T. F. *Science* **2005**, *308*, 838–841.

(5) Misewich, J. A.; Martel, R.; Avouris, P.; Tsang, J. C.; Heinze, S.; Tersoff, J. *Science* **2003**, *300*, 783–786.

(6) Wildoer, J. W. G.; Venema, L. C.; Rinzler, A. G.; Smalley, R. E.; Dekker, C. *Nature* **1998**, *391*, 59–62.

(7) Odom, T. W.; Huang, J. L.; Kim, P.; Lieber, C. M. *Nature* **1998**, *391*, 62–64.

(8) Dai, H. J.; Wong, E. W.; Lieber, C. M. *Science* **1996**, *272*, 523–526.

(9) Bockrath, M.; Cobden, D. H.; McEuen, P. L.; Chopra, N. G.; Zettl, A.; Thess, A.; Smalley, R. E. *Science* **1997**, *275*, 1922–1925.

(10) Tans, S. J.; Verschueren, A. R. M.; Dekker, C. *Nature* **1998**, *393*, 49–52.

(11) Baughman, R. H.; Zakhidov, A. A.; de Heer, W. A. *Science* **2002**, *297*, 787–792.

(12) Liang, W. J.; Bockrath, M.; Bozovic, D.; Hafner, J. H.; Tinkham, M.; Park, H. *Nature* **2001**, *411*, 665–669.

(13) Ajayan, P. M.; Stephan, O.; Colliex, C.; Trauth, D. *Science* **1994**, *265*, 1212–1214.

(14) Baughman, R. H.; Cui, C. X.; Zakhidov, A. A.; Iqbal, Z.; Barisci, J. N.; Spinks, G. M.; Wallace, G. G.; Mazzoldi, A.; De Rossi, D.; Rinzler, A. G.; Jaschinski, O.; Roth, S.; Kertesz, M. *Science* **1999**, *284*, 1340–1344.

(15) Kim, P.; Lieber, C. M. *Science* **1999**, *286*, 2148–2150.

(16) Tombler, T. W.; Zhou, C. W.; Alexseyev, L.; Kong, J.; Dai, H. J.; Lei, L.; Jayanthi, C. S.; Tang, M. J.; Wu, S. Y. *Nature* **2000**, *405*, 769–772.

(17) Yu, M. F.; Files, B. S.; Arepalli, S.; Ruoff, R. S. *Phys. Rev. Lett.* **2000**, *84*, 5552–5555.

(18) Iijima, S.; Ichihashi, T. *Nature* **1993**, *363*, 603–605.

(19) Bethune, D. S.; Klang, C. H.; de Vries, M. S.; Gorman, G.; Savoy, R.; Vazquez, J.; Beyers, R. *Nature* **1993**, *363*, 605–607.

(20) Thess, A.; Lee, R.; Nikolaev, P.; Dai, H.; Petit, P.; Robert, J.; Xu, C.; Lee, Y. H.; Kim, S. G.; et al. *Science* **1996**, *273*, 483–487.

(21) Girifalco, L. A.; Hodak, M.; Lee, R. S. *Phys. Rev. B* **2000**, *62*, 13104–13110.

(22) Bandow, S.; Rao, A. M.; Williams, K. A.; Thess, A.; Smalley, R. E.; Eklund, P. C. *J. Phys. Chem. B* **1997**, *101*, 8839–8842.

(23) Tasis, D.; Tagmatarchis, N.; Bianco, A.; Prato, M. *Chem. Rev.* **2006**, *106*, 1105–1136.

(24) Tang, B. Z.; Xu, H. Y. *Macromolecules* **1999**, *32*, 2569–2576.

(25) O'Connell, M. J.; Boul, P.; Ericson, L. M.; Huffman, C.; Wang, Y.; Haroz, E.; Kuper, C.; Tour, J.; Ausman, K. D.; Smalley, R. E. *Chem. Phys. Lett.* **2001**, *342*, 265–271.

(26) Star, A.; Steuerman, D. W.; Heath, J. R.; Stoddart, J. F. *Angew. Chem., Int. Ed.* **2002**, *41*, 2508–2512.

(27) Star, A.; Gabriel, J. C. P.; Bradley, K.; Gruner, G. *Nano Lett.* **2003**, *3*, 459–463.

(28) Zheng, M.; Jagota, A.; Semke, E. D.; Diner, B. A.; McLean, R. S.; Lustig, S. R.; Richardson, R. E.; Tassi, N. G. *Nat. Mater.* **2003**, *2*, 338–342.

(29) Coleman, J. N.; Curran, S.; Dalton, A. B.; Davey, A. P.; McCarthy, B.; Blau, W.; Barklie, R. C. *Phys. Rev. B* **1998**, *58*, R7492–R7495.

(30) Coleman, J. N.; Curran, S.; Dalton, A. B.; Davey, A. P.; Mc Carthy, B.; Blau, W.; Barklie, R. C. *Synth. Met.* **1999**, *102*, 1174–1175.

(31) Park, C.; Ounaies, Z.; Watson, K. A.; Crooks, R. E.; Smith, J.; Lowther, S. E.; Connell, J. W.; Siochi, E. J.; Harrison, J. S.; Clair, T. L. S. *Chem. Phys. Lett.* **2002**, *364*, 303–308.

(32) Pinto, N. J.; Johnson, A. T.; MacDiarmid, A. G.; Mueller, C. H.; Theofylaktos, N.; Robinson, D. C.; Miranda, F. A. *Appl. Phys. Lett.* **2003**, *83*, 4244–4246.

(33) Freitag, M.; Martin, Y.; Misewich, J. A.; Martel, R.; Avouris, P. H. *Nano Lett.* **2003**, *3*, 1067–1071.

(34) Panhuis, M. I. H.; Maiti, A.; Dalton, A. B.; van den Noort, A.; Coleman, J. N.; McCarthy, B.; Blau, W. J. *J. Phys. Chem. B* **2003**, *107*, 478–482.

(35) Chen, J.; Liu, H. Y.; Weimer, W. A.; Halls, M. D.; Waldeck, D. H.; Walker, G. C. *J. Am. Chem. Soc.* **2002**, *124*, 9034–9035.

(36) Rice, N. A.; Soper, K.; Zhou, N.; Merschrod, E.; Zhao, Y. *Chem. Commun.* **2006**, 4937–4939.

(37) Nish, A.; Hwang, J.-Y.; Doig, J.; Nicholas, R. J. *Nat. Nanotechnol.* **2007**, *2*, 640–646.

(38) Hwang, J.-Y.; Nish, A.; Doig, J.; Douven, S.; Chen, C.-W.; Chen, L.-C.; Nicholas, R. J. *J. Am. Chem. Soc.* **2008**, *130*, 3543–3553.

(39) Kang, Y. K.; Deria, P.; Carroll, P. J.; Therien, M. J. *Org. Lett.* **2008**, *10*, 1341–1344.

(40) Moore, V. C.; Strano, M. S.; Haroz, E. H.; Hauge, R. H.; Smalley, R. E.; Schmidt, J.; Talmon, Y. *Nano Lett.* **2003**, *3*, 1379–1382.

(41) Zorbas, V.; Ortiz-Acevedo, A.; Dalton, A. B.; Yoshida, M. M.; Dieckmann, G. R.; Draper, R. K.; Baughman, R. H.; Jose-Yacaman, M.; Musselman, I. H. *J. Am. Chem. Soc.* **2004**, *126*, 7222–7227.

(42) Paloniemi, H.; Aaritalo, T.; Laiho, T.; Liuke, H.; Kocharova, N.; Haapakka, K.; Terzi, F.; Seeber, R.; Lukkari, J. *J. Phys. Chem. B* **2005**, *109*, 8634–8642.

(43) Minami, N.; Kim, Y.; Miyashita, K.; Kazaoui, S.; Nalini, B. *Appl. Phys. Lett.* **2006**, *88*, 093123.

(44) Matarredona, O.; Rhoads, H.; Li, Z. R.; Harwell, J. H.; Balzano, L.; Resasco, D. E. *J. Phys. Chem. B* **2003**, *107*, 13357–13367.

(45) While the concentration of PPES will play a role in determining these values, note that these PPES-SWNT preparations utilized a 3.5 mM (∼0.15%) PPES solution (Supporting Information). For the preparation of SDS-SWNTs, we used a 7.0 mM (∼0.2%) SDS solution; this was based on an optimum concentration described in the literature.[44] The reported mass percent conversion values for a number of representative SWNT dispersions are ∼40, 64, and 83%, for respective ssDNA-,[28] SDBS-,[44] and NaCMC-based surfactants.[43] Note that the respective initial surfactant concentrations used to obtain the above-noted mass-percent conversions were ca. 0.1, 0.12, and 1% for ssDNA, SDBS, and NaCMC.

(46) Weisman, R. B. *Applied Physics of Carbon Nanotubes: Fundamentals of Theory, Optics and Transport Devices*; Springer: New York, 2005; pp 183−202.

(47) Weisman, R. B.; Bachilo, S. M. *Nano Lett.* **2003**, *3*, 1235–1238.

(48) The peaks centered at 976, 1020, 1055 nm in the SDS-SWNT sample can be unambiguously assigned to optical transitions of the first subband for (6,5), (7,5), and (10,2) tubes, respectively.[2] These peaks are respectively shifted to 994, 1041, 1075 nm in the PPES-SWNT sample prepared using a 30 min sonication time, and respectively to 993, 1039, 1073 nm when the sonication time was fixed at 3 h.

(49) Jeng, E. S.; Moll, A. E.; Roy, A. C.; Gastala, J. B.; Strano, M. S. *Nano Lett.* **2006**, *6*, 371–375.

(50) Phillips, J. C.; Braun, R.; Wang, W.; Gumbart, J.; Tajkhorshid, E.; Villa, E.; Chipot, C.; Skeel, R. D.; Kale, L.; Schulten, K. *J. Comput. Chem.* **2005**, *26*, 1781–1802.

(51) MacKerell, A. D.; Bashford, D.; Bellott, M.; Dunbrack, R. L.; Evanseck, J. D.; Field, M. J.; Fischer, S.; Gao, J.; Guo, H.; Ha, S.; Joseph-McCarthy, D.; Kuchnir, L.; Kuczera, K.; Lau, F. T. K.; Mattos, C.; Michnick, S.; Ngo, T.; Nguyen, D. T.; Prodhom, B.; Reiher, W. E.; Roux, B.; Schlenkrich, M.; Smith, J. C.; Stote, R.; Straub, J.; Watanabe, M.; Wiorkiewicz-Kuczera, J.; Yin, D.; Karplus, M. *J. Phys. Chem. B* **1998**, *102*, 3586–3616.

(52) This experimentally observed repeating structural characteristic for helical wrapping by PPES is also observed for two-tube bundles (Supporting Information, Figure S6b) and other modestly sized SWNT bundle aggregates (Supporting Information, Figure S6c), suggesting this structural motif is the major interaction mode, regardless of tube or bundle size. Note that the observed helical pitch in these PPES-wrapped SWNT bundles tracks predictably with bundle size.

(53) Numata, M.; Asai, M.; Kaneko, K.; Bae, A. H.; Hasegawa, T.; Sakurai, K.; Shinkai, S. *J. Am. Chem. Soc.* **2005**, *127*, 5875–5884.

NL8032334